

# Comparing hierarchical black hole mergers in star clusters and active galactic nuclei

GUO-PENG LI<sup>1</sup> AND DA-BIN LIN<sup>1</sup><sup>1</sup>*Guangxi Key Laboratory for Relativistic Astrophysics, School of Physical Science and Technology, Guangxi University, Nanning 530004, China*

## ABSTRACT

Star clusters (SCs) and active galactic nuclei (AGNs) are promising sites for the occurrence of hierarchical black hole (BH) mergers. We use simple models to compare hierarchical BH mergers in two of the dynamical formation channels. We find that the primary mass distribution of hierarchical mergers in AGNs is higher than that in SCs, with the peaks of  $\sim 50 M_{\odot}$  and  $\sim 13 M_{\odot}$ , respectively. The effective spin ( $\chi_{\text{eff}}$ ) distribution of hierarchical mergers in SCs is symmetrical around zero as expected and  $\sim 50\%$  of the mergers have  $|\chi_{\text{eff}}| > 0.2$ . The distribution of  $\chi_{\text{eff}}$  in AGNs is narrow and prefers positive values with the peak of  $\chi_{\text{eff}} \geq 0.3$  due to the assistance of AGN disks. BH hierarchical growth efficiency in AGNs, with at least  $\sim 30\%$  of mergers being hierarchies, is much higher than the efficiency in SCs. In addition, there are obvious differences in the mass ratios and effective precession parameters of hierarchical mergers in SCs and AGNs. We argue that the majority of the hierarchical merger candidates detected by LIGO-Virgo may originate from the AGN channel as long as AGNs get half of the hierarchical merger rate.

**Keywords:** Gravitational waves; Stellar mass black holes; Star clusters; Active galactic nuclei

## 1. INTRODUCTION

Likely, at least one binary black hole (BBH) merger event in the gravitational-wave transient catalog (GWTC, Abbott et al. 2021; The LIGO Scientific Collaboration et al. 2021a) reported by the LIGO-Virgo-KAGRA (LVK) Collaboration is a hierarchical merger (Kimball et al. 2021; Mould et al. 2022). Hierarchical mergers are expected to occur in dense stellar environments such as star clusters (SCs, e.g., nuclear star clusters, NSCs and globular clusters, GCs) and active galactic nuclei (AGNs) (Gerosa & Fishbach 2021).

A second-generation (2G) black hole (BH) formed by merging a 1G BBH formed from the collapse of stars can be retained by the host if the escape speed of the host stands larger than its kick recoil velocity imparted by the loss of linear momentum. Then, the 2G BH will pair with another BH to form a 2G BBH, merge within a Hubble time, and therefore produce a 3G BHs. Repeatedly, there might be the occurrence of higher-generation mergers. Hierarchical mergers have been extensively discussed in SCs (e.g., Rodríguez et al. 2019; Kimball et al. 2020, 2021; Baibhav et al. 2021; Mapelli et al. 2021a,b; Li

2022a) and AGNs (e.g., Yang et al. 2019b; Gayathri et al. 2020; Tagawa et al. 2021b; Li 2022b), which can efficiently pollute the pair-instability (PI) mass gap (between  $\sim 50$ – $120 M_{\odot}$ ) predicted by PI supernovae (Heger et al. 2003) and Pulsational PI supernovae (Woosley et al. 2007). It is also an alternate pathway to explain the growth of intermediate-mass black holes (IMBHs) in dense stellar environments (Quinlan & Shapiro 1987; Fragione et al. 2020, 2022; González Prieto et al. 2022).

Zevin & Holz (2022) studied the retention efficiency of BBH merger remnants in dense stellar clusters by considering three hierarchical merger branches: NG+1G, NG+NG, and NG+ $\leq$ NG (NG refers to the BH generation). By seeding, growing, and pruning the three hierarchical branches, they found that if escape velocities reach  $\sim 300 \text{ km s}^{-1}$ , then the fraction of detectable hierarchical mergers with a source-frame total mass of  $\geq 100 M_{\odot}$  will exceed the observed upper limit of the LVK analysis (The LIGO Scientific Collaboration et al. 2021b). Therefore, they stressed that some unknown mechanisms are needed to avoid a ‘cluster catastrophe’ of overproducing BBH mergers if such environments dominate the BBH merger rate.

NG+1G mergers are expected to preferentially occur in AGNs because of migration traps in high-density gas disks within about 300 Schwarzschild radii from the central supermassive BH (McKernan et al. 2012; Bellovary et al. 2016;

Secunda et al. 2019). Because the merger remnants could continue to reside in migration traps and merge again with another 1G BH that aligned with the AGN disk and migrated to traps within the disk (McKernan et al. 2018; Yang et al. 2019b; Li 2022b). While the occurrence of NG+NG mergers is preferentially in SCs because of mass segregation (e.g., Scaria & Bappu 1981; Nony et al. 2021; Pavlík & Vesperini 2022; Vitral et al. 2022). Because more massive NG BHs would concentrate on the dense core of SCs, where they will preferentially form NG+NG binaries in dynamical interactions (Rodríguez et al. 2019). NG+≤NG mergers include but are not limited to the mergers of NG+1G and NG+NG, which is representative of a steady-state limit (Zevin & Holz 2022).

Previous studies focused on hierarchical BH mergers in a single formation channel or multiple channels without AGNs (e.g., Gerosa & Berti 2019; Rodríguez et al. 2019; Yang et al. 2019b; Fragione & Silk 2020; Liu & Lai 2021; Mapelli et al. 2021a,b; Mahapatra et al. 2021, 2022; Li 2022a,b; Zevin & Holz 2022, but Doctor et al. 2020; Tagawa et al. 2021a). In this paper, we compare hierarchical BH mergers in SCs and AGNs using simple models that are similar in construction to previous work (Gerosa et al. 2021; Tagawa et al. 2021a; Zevin & Holz 2022; Mahapatra et al. 2022). Because hybrid Monte Carlo and/or N-body simulations of dense stellar environments are extremely difficult to investigate the relevant parameter space of hierarchical mergers due to the computational cost. The rest of this paper is organized as follows. In Section 2 we describe our model framework. In Section 3 we show our results in both SCs and AGNs. Finally, in Section 4 we discuss our assumptions, and escape velocities and delay times, and we conclude with implications in Section 5.

## 2. MODELS

Following Zevin & Holz (2022), we consider three hierarchical BBH merger branches: NG+1G, NG+NG, and NG+≤NG. We use numerical relativity fits to calculate each merger remnant’s total mass (Barausse et al. 2012), spin (Hofmann et al. 2016), and kick velocity (Campanelli et al. 2007) (see also some summaries of Gerosa & Kesden 2016 and Mahapatra et al. 2021). Table 1 lists the summary of our models.

### 2.1. First-generation BHs

We adopt a 1G BH mass distribution in dense stellar environments as  $p(m) \propto m^{-\alpha}$ . The range of BH masses  $m \in [5 M_{\odot}, 50 M_{\odot}]$  is adopted, which is determined by the lower and PI mass gap. We adopt  $\alpha = 2.3$  in SCs corresponding to the Kroupa initial mass function (Kroupa 2001);  $\alpha = 1$  within AGN disks because the disks harden the initial BH mass function (Yang et al. 2019a).

We assume a uniform spin magnitude distribution:  $U(0, \chi_{\max})$  with  $\chi_{\max} = 0.2$  in SCs (The LIGO Scientific Collaboration et al. 2021b). Spin tilt angles for all BH generations are isotropically drawn over a sphere. However, the spin of BHs in AGN disks may be significantly altered under accretion; spin magnitudes are going to be higher overall (Yi & Cheng 2019; McKernan et al. 2020), and the misalignment angle  $\theta$  between the spin and the orbital angular momenta changed with  $\cos\theta \rightarrow 1$  or  $-1$  (Yi & Cheng 2019). Whereas the vast majority should have  $\theta \leq \pi/2$  because gas accretion from AGN disks will tend to torque the BH spin into alignment with the gas after about 1%–10% of the gas accreted and after 10 Myr any BHs that have been present in the disk should have been torqued into alignment with the disk orbital angular momentum (Bogdanović et al. 2007). For simplicity, we neglect the case of  $\cos\theta < 0$ , which should be a very few part and not make a difference to our results. Therefore, we adopt  $\chi_{\max} = 0.4$ , and  $\cos\theta$  between 0 and 1 according to a distribution uniform in  $p(\cos\theta) \propto \cos\theta$  in AGN disks. We also adopt  $\chi_{\max} = 0.01$  and  $0.4$  and  $\chi_{\max} = 0.2$  and  $1$  in SCs and AGN disks, respectively, for comparison.

We draw the primary component BH mass ( $m_1$ ) of a 1G binary (i.e., 1G+1G) according to the above distributions. Then, we pair it with another component BH according to  $m_2 = m_1 q$  ( $m_1 \geq m_2 \geq 5 M_{\odot}$ ,  $q$  is the mass ratio of a BBH) with  $p(q) \propto q^{\beta}$ , and adopt  $q$  between the bounds  $[0.3, 1]$ . We consider two values for  $\beta$ : 1.08 for SCs and 0 for AGNs.  $\beta \sim 1.08$  is inferred from the GWTC-3 by the LVK Collaboration (The LIGO Scientific Collaboration et al. 2021b).  $\beta = 0$  represents random pairing, which is expected in AGN disks because of runaway mergers in migration traps (Yang et al. 2019b; Li 2022b). We also consider  $\beta = 5$  for SCs indicating ‘strong’ mass segregation, and we adopt  $\beta = 1.08$  for AGN disks for comparison if migration traps are inefficient.

We note that a predictively initial BH mass distribution from the Power Law + Peak model of The LIGO Scientific Collaboration et al. (2021b) is also considered by Zevin & Holz (2022). The difference between these two distributions is the latter allows BH masses to be in the PI mass gap because it probably includes merger remnants, which means it is not representative of a true distribution of 1G black hole masses. Therefore, we do not consider it in our models. Mahapatra et al. (2022) considered  $\beta = -1$  that prefers asymmetric binaries, although it is in disfavor of the observed results. However, they have shown that if the pairing prefers equal-mass binaries, then 2G and 3G mergers are consistent with two of the subdominant peaks of the predictive BH mass spectrum from the Flexible Mixture model (Tiwari 2021, 2022).

### 2.2. Constraining Hierarchical Growth Efficiency

**Table 1.** Summary of the models.

Model	$\alpha$	$\chi_{\max}$	Spin direction	$\beta$	$V_{\text{esc}}$ [km s <sup>-1</sup> ]	$t_{\min}$ [Myr]
SC_1	2.3	0.2	Isotropic	1.08	100	10
SC_2	2.3	0.2	Isotropic	1.08	50	10
SC_3	2.3	0.2	Isotropic	1.08	200	10
SC_4	2.3	0.2	Isotropic	1.08	300	10
SC_5	2.3	0.2	Isotropic	1.08	500	10
SC_6	2.3	0.2	Isotropic	1.08	100	0.1
SC_7	2.3	0.2	Isotropic	1.08	100	100
SC_8	2.3	0.2	Isotropic	5	100	10
SC_9	2.3	0.01	Isotropic	1.08	100	10
SC_10	2.3	0.4	Isotropic	1.08	100	10
AGN_1	1	0.4	Anisotropic	0	$\infty$	0.1
AGN_2	1	0.4	Anisotropic	0	$10^3$	0.1
AGN_3	1	0.4	Anisotropic	0	$\infty$	0.01
AGN_4	1	0.4	Anisotropic	0	$\infty$	1
AGN_5	1	0.4	Anisotropic	0	$\infty$	2
AGN_6	1	0.4	Anisotropic	1.08	$\infty$	0.1
AGN_7	1	0.2	Anisotropic	0	$\infty$	0.1
AGN_8	1	1	Anisotropic	0	$\infty$	0.1

Column 1: Name of the model. ‘SC\_’ represents the SC-like environment; ‘AGN\_’ represents the AGN-like environment. Column 2: The mass index  $\alpha$ . Column 3: The maximum initial spin  $\chi_{\max}$ . Column 4: The spin direction for all BH generations. ‘Isotropic’ represents spin tilt angles are isotropically drawn over a sphere; ‘Anisotropic’ represents the misalignment angle  $\theta$  obeying a distribution uniform in  $p(\cos\theta) \propto \cos\theta$  spanning from 0 and 1. Column 5: The mass-ratio index  $\beta$ . Column 6: The escape velocity  $V_{\text{esc}}$ .  $V_{\text{esc}} = \infty$  represents that the kicks of merger remnants are neglected. Column 7: The delay times  $\Delta t$  between the subsequent mergers.

We constrain the growth efficiency of hierarchical mergers by escape velocities, delay times, and merger generations.

- We drop all subsequent mergers if  $V_{\text{kick}} \geq V_{\text{esc}}$ , where  $V_{\text{kick}}$  is the kick velocity of the merger remnant and  $V_{\text{esc}}$  is the escape velocity of the host. The kick velocities inferred from the GWTC events can lie in a wide range:  $\sim 50\text{--}2000$  km s<sup>-1</sup> (Mahapatra et al. 2022; Varma et al. 2022). In comparison, the escape speed is  $\sim 2\text{--}100$  km s<sup>-1</sup> for GCs (Antonini & Rasio 2016),  $\sim 10\text{--}600$  km s<sup>-1</sup> for NSCs (Antonini & Rasio 2016), and up to  $\sim 1000$  km s<sup>-1</sup> in AGN disks within an inner radii. The kicks of merger remnants in AGNs are generally neglected by the previous works (Tagawa et al. 2020; Yang et al. 2020; Li 2022b), because of the large orbital velocities  $\sim 2 \times 10^4$  km s<sup>-1</sup> and the small kick magnitude due to BH spins are largely aligned or anti-aligned with the disk (McKernan et al. 2020).
- BBH mergers can occur before the present day. We draw the delay times between the subsequent mergers according to a distribution uniform in  $p(\Delta t) \propto \Delta t^{-1}$  with  $\Delta t = t_{N_{\text{merg}}+1} - t_{N_{\text{merg}}}$  (Dominik et al. 2012). For SCs, we span  $\Delta t$  from  $t_{\min} = 10$  Myr to  $t_{\max} = 1.4 \times 10^4$  Myr (Di Carlo et al. 2020; Zevin & Holz 2022). The time efficiency of BBH formation and merger is

significantly high under the assistance of AGN disks. In AGN disks, the characteristic time of the migration for BHs is  $10^5$  yr (McKernan et al. 2012; Bartos et al. 2017), which is also much larger than the merger time of  $\lesssim 10^4$  yr (Bartos et al. 2017; Secunda et al. 2019). We assume that delay times in AGN disks spanning from  $t_{\min} = 0.1$  Myr to  $t_{\max} = 10$  Myr. For comparison, we also adopt that  $t_{\min} = 0.1$  Myr and 100 Myr for SCs (Mapelli et al. 2021a) and  $t_{\min} = 0.01$  Myr, 1 Myr, and 2 Myr for AGNs. We discard the mergers that occurred 10 Myr later in AGNs.

- Higher-generation mergers are rarer than lower-generation mergers. In AGNs, the fraction of hierarchical mergers is the highest, namely  $\sim 20\text{--}50\%$  (Yang et al. 2019b; McKernan et al. 2020; Li 2022b), because BBHs merge and remain near migration traps, enabling the merger remnants to merge with additional BHs. Therefore, the hierarchical merger generation in AGNs can reach up to 5G. While the percentage in SCs is  $\lesssim 30\%$  because of the relatively low retention probability of merger remnants, especially in GCs (Rodríguez et al. 2019; Mapelli et al. 2021a,b; Li 2022a). Thus, the maximum generation of hierarchical mergers in SCs might be  $\leq 3$ G. Here, we use a maxi-

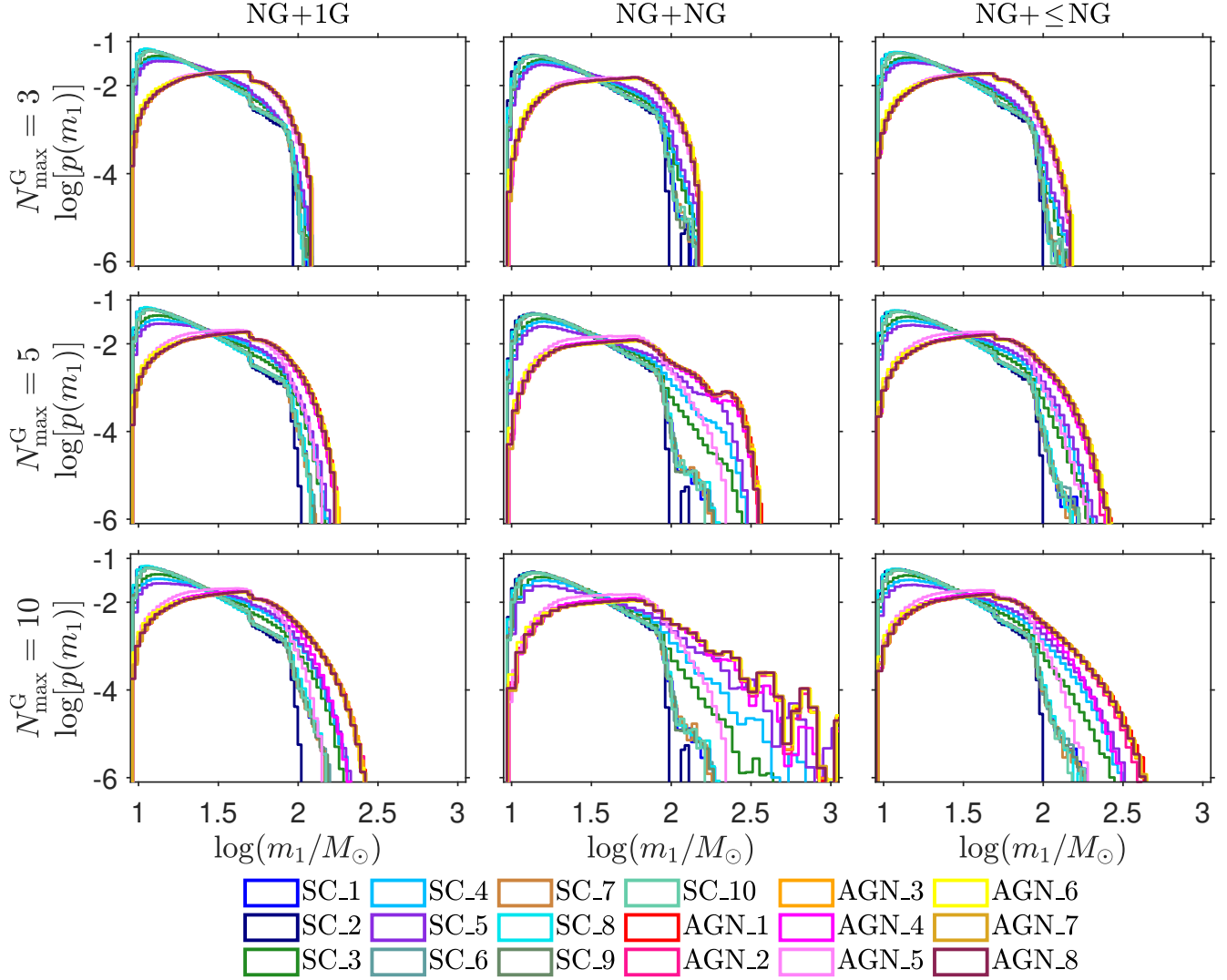


**Figure 1.** The probability density distribution of the primary masses ( $m_1$ ) of hierarchical BH mergers. The columns show the three hierarchical branches (i.e., NG+1G, NG+NG, and NG+ $\leq$ NG), and the rows show the three different maximum merger generations (i.e.,  $N_{\max}^G = 3, 5$ , and 10). The different lines in each pixel show the eighteen models listed in Table 1. Each line plotted contains the contributions of all hierarchical merger generations and the fraction of each merger generation is obtained from Table 2 in Appendix A.

merger generation  $N_{\max}^G$  to constrain the hierarchical growth efficiency with  $N_{\max}^G = 3, 5$ , and 10. We note that Zevin & Holz (2022) constrained hierarchical mergers using BH budget being the 1G BH number required in a hierarchical chain, which the effect is the same as if we use  $N_{\max}^G$ . Meanwhile, we constrain the fraction of mergers with generation  $N$  to  $f(N) \leq 2^{-N}$ . For example, there has at most 100 2G mergers and 50 3G mergers if only 200 1G mergers occur. The merger generation with  $N$  contains  $N$  merger types: NG+1G, NG+2G, ..., and NG+NG.

### 2.3. Synthesizing Hierarchical Mergers

We first produce  $N_{1G} = 10^6$  1G BHs according to the previously described mass distributions and spin distributions and

pair them according to the previously described mass-ratio distribution. We calculate their kick velocities and merger times to select the remnants (i.e., 2G BHs) with the number of  $N_{2G} = N_{1G} - N'_{1G}$  that were retained by the host and occurred before the present day. We randomly pair these 2G BHs with 1G BH population and 2G BH population for NG+1G and NG+NG mergers, respectively. For NG+ $\leq$ NG mergers, we pair each 2G BH with a BH with the generation  $M$  ( $M \leq N$ ). The probability of the generation  $M$  obeys  $p(M) \propto 2^{-(M-1)}$ . We repeat the above method to obtain the higher-generation merger population and stop our iteration when the maximum merger generation is up to  $N_{\max}^G$ .

## 3. RESULTS

### 3.1. Mass Distribution

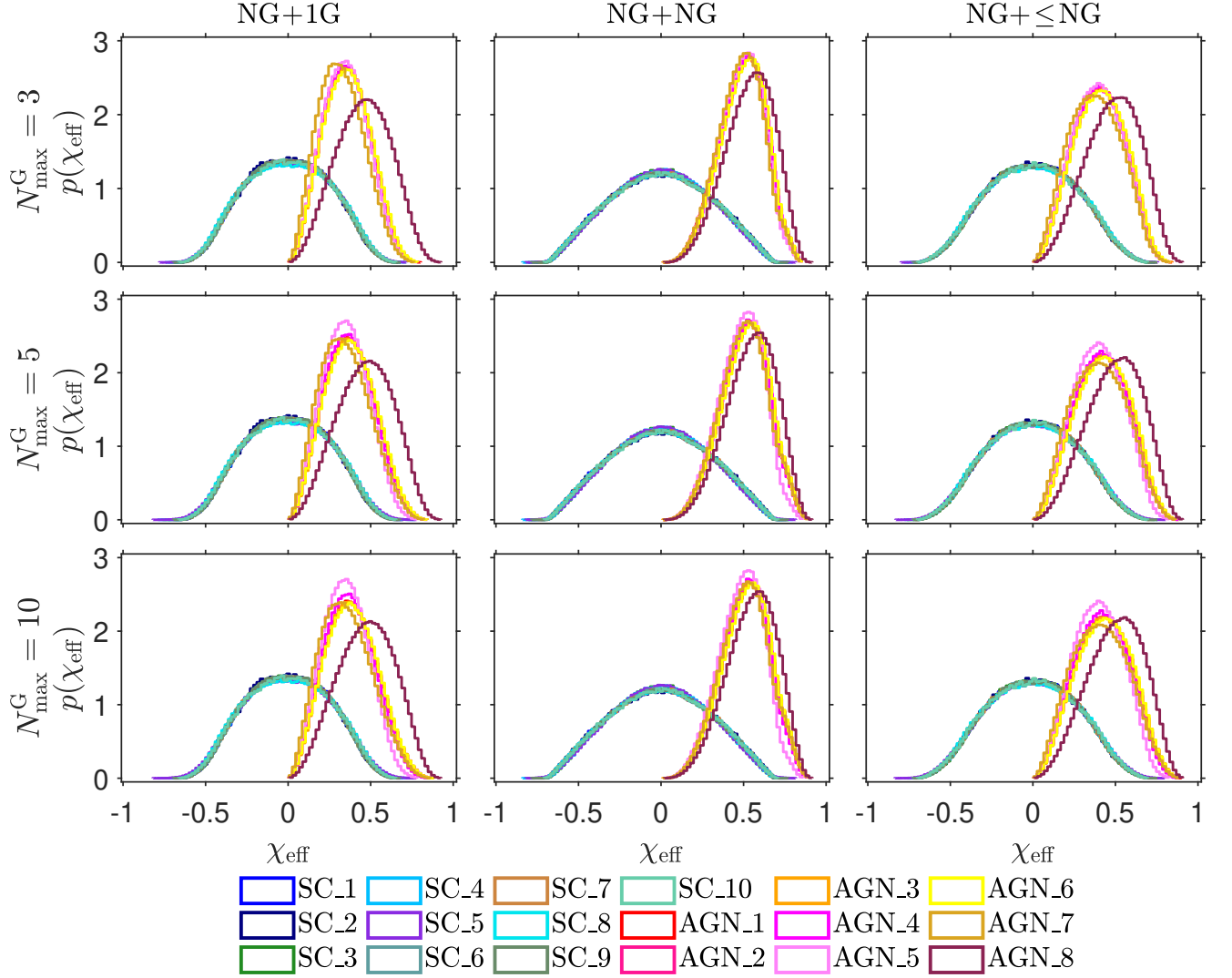


**Figure 2.** Same as Figure 1, but the probability density distribution of the effective spins ( $\chi_{\text{eff}}$ ) of hierarchical BH mergers.

We show the primary BH mass distribution of hierarchical mergers (i.e., excluding 1G mergers) in Figure 1. There is a distinct difference between the masses of hierarchical mergers in SCs and AGNs, in which the distributions with wide ranges in AGNs are higher than that in SCs due to the hard initial mass spectrum and efficient hierarchical mergers (see Table 2 in Appendix A). The peaks of the distributions in SCs are  $\sim 11\text{--}15 M_{\odot}$  as similar with Mahapatra et al. (2022), while that in AGNs can reach up to  $\sim 50 M_{\odot}$  being consistent with Yang et al. (2019b). The NG+1G mergers have relatively low masses because one of each of them came from a 1G BH that has a mass of  $\leq 50 M_{\odot}$ . Whereas the NG+NG mergers have relatively high masses because the binaries are in favor of symmetric masses. As the maximum merger generation increases, the high-mass end of the distributions gradually rises.

We find that the hierarchical mergers for all the different cases can efficiently pollute the PI mass gap, but it is difficult to build up IMBHs for the cases with the maximum merger generation  $N_{\text{max}}^G = 3$ . However, that in AGNs seem to be the best choice for both the PI mass gap and IMBHs due to the relatively high mass distribution; especially its BBH merger rate may exceed the merger rate in NSCs (Saavik Ford & McKernan 2022).

We see that the escape velocities play an important role for hierarchical merges in SCs. The small escape velocity represents the inefficiency of hierarchical merges, which causes low merger masses; the larger the escape velocity, the higher the masses. When  $N_{\text{max}}^G = 10$ , the high-mass end of the distributions for the cases with different escape velocities has significant differences; in particular, the masses of the NG+NG mergers can reach up to  $\sim 1000 M_{\odot}$ . Moreover, the pairing



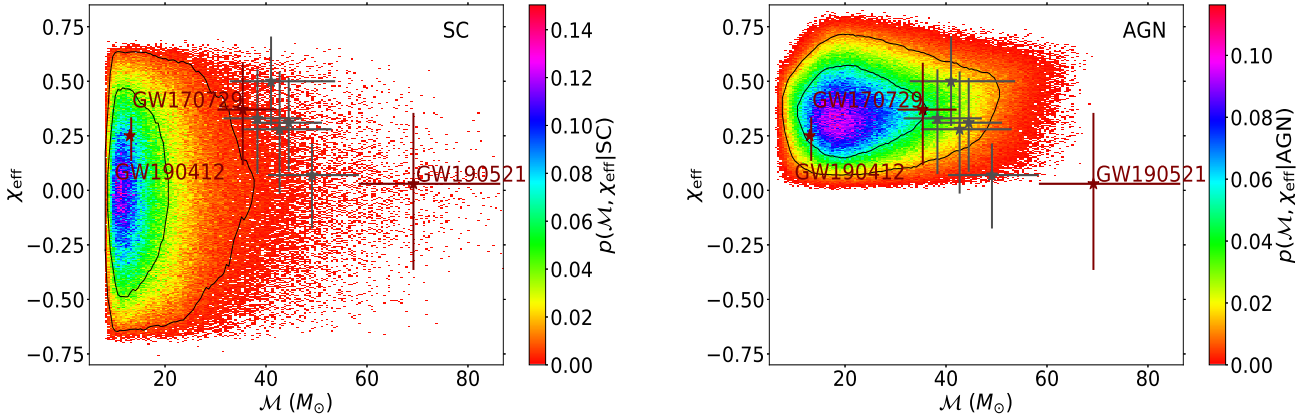


**Figure 3.** 2D probability densities of the chirp mass ( $\mathcal{M}$ ) and effective spin ( $\chi_{\text{eff}}$ ) of hierarchical BH mergers in SCs (left) and AGNs (right). The two fiducial models (i.e., SC\_1 and AGN\_1) are adopted for SCs and AGNs, respectively. The black solid lines show 50% and 90% confidence regions. The maximum merger generations  $N_{\text{max}}^G = 3$  and 5 and the hierarchical branches with NG+NG and NG+1G are assumed in SCs and AGNs, respectively. Because we expect that the mergers of NG+NG and NG+1G dominate the hierarchical merger rates in SCs and AGNs, respectively, and that hierarchical merger growth efficiency in AGNs is higher than that in SCs. We also show eight promising GW candidate events (star symbols) for hierarchical mergers, in which GW170729 (Abbott et al. 2019), GW190412 (Abbott et al. 2020a), and GW190521 (Abbott et al. 2020b) are highlighted.

probability of  $\beta = 5$  (SC-8) could upraise the mass distribution at the high-mass end.

For the hierarchical merges in AGNs, the mass distributions for all the different cases (excluding AGN\_5) are no significant differences. Because all the mergers could be retained in migration traps, and the delay times are relatively short with the assistance of AGN disks, resulting in almost the same fraction in the same merger generation for the different model (see Table 2 in Appendix A). This also results in  $\sim 30\text{--}50\%$  of the merging BBHs being hierarchical mergers.

### 3.2. Spin Distribution

In Figure 2, we plot the probability density distribution of the effective spins ( $\chi_{\text{eff}}$ ) of hierarchical BH mergers.  $\chi_{\text{eff}} = (m_1\chi_1\cos\theta_1 + m_2\chi_2\cos\theta_2)/(m_1 + m_2)$ , where  $m_i$ ,  $\chi_i$ , and  $\theta_i$  are the mass, the dimensionless spin, and the misalignment angle, respectively, of each BH in a merged BBH.

We see that the distributions in SCs are symmetrical around zero as expected due to random spin directions. However, they have a wide range from  $\sim -0.75$  to  $\sim 0.75$  with  $\sim 50\%$  of the mergers have  $|\chi_{\text{eff}}| \geq 0.2$  because the final spins of 1G mergers concentrate on 0.69, which the similar results were obtained by Rodriguez et al. (2019) and Mapelli et al. (2021b). The distributions with the peaks of  $\chi_{\text{eff}} \geq 0.3$  in AGNs are narrower and always greater than 0 because we assume that the misalignment angles of the BBHs are less than  $\pi/2$ . The reason for this assumption is that gas accretion from the AGN disk will tend to torque the BH spin direction into alignment with the disk orbital angular momentum (Bogdanović et al. 2007).

We find that there are no differences between  $\chi_{\text{eff}}$  either in SCs or in AGNs if variations to both the hierarchical branch

and the maximum merger generation are fixed because the finally spins of any merger generations ( $N \leq 10$ ) lie in a stable range from  $\sim 0.5$  to  $\sim 0.8$  (Gerosa et al. 2021; Zevin & Holz 2022). That indicates that the effective spin distribution of hierarchical mergers weakly depends on escape velocities and delay times. In SCs, the distribution of  $\chi_{\text{eff}}$  of NG+NG mergers is relatively wider than that of the other two hierarchical branches, though not obvious. In AGNs, the peaks of the distributions of  $\chi_{\text{eff}}$  of the mergers of NG+1G, NG+ $\leq$ NG, NG+NG increase in turn to  $\sim 0.32$ ,  $\sim 0.4$ , and  $\sim 0.5$ , respectively, which means equal-mass BBH mergers have large effective spins. The peak values of the distributions in AGNs broadly agree with the distributions of the 2G and 3G mergers in Yang et al. (2019b).

Figure 2 also shows that the gravitational-wave (GW) events with large  $\chi_{\text{eff}}$  reported by LVK (The LIGO Scientific Collaboration et al. 2021a) most likely originate from AGNs because  $\chi_{\text{eff}}$  of the merger from isolated binary evolution tend to be positive close to zero, while that from SCs centers zero (see also Figure 3). The distribution of the model of AGN\_8 is higher than others because we adopt the maximum initial BH spin is 1.

### 3.3. Comparison with the Promising Candidates

We would expect that NG+1G and NG+NG mergers dominate the hierarchical BH merger rates in AGNs and SCs, respectively, because of migration traps and mass segregation. We show 2D probability densities of the chirp mass ( $\mathcal{M} = (m_1m_2)^{3/5}/(m_1 + m_2)^{1/5}$ ) and effective spin ( $\chi_{\text{eff}}$ ) of the hierarchical BH mergers in SCs and AGNs in Figure 3. In the left panel, we plot the hierarchical mergers in SCs with the model of SC\_1, the hierarchical branch of NG+NG

and  $N_{\text{max}}^G = 3$ , and in the right is the hierarchical mergers in AGNs with the model of AGN<sub>L</sub>1, the hierarchical branch of NG+1G and  $N_{\text{max}}^G = 5$ .  $N_{\text{max}}^G = 5$  adopted is because it contains at least 99% of the hierarchical mergers in AGNs (Yang et al. 2019b; Li 2022b). We see that the distribution with the densest region located at  $M \sim 11 M_\odot$  and  $\chi_{\text{eff}} \sim 0$  in SCs has a wider range than that with the densest region located at  $M \sim 20 M_\odot$  and  $\chi_{\text{eff}} \sim 0.4$  in AGNs.

Kimball et al. (2021) found evidence for hierarchical mergers in the GWTC-2 (Abbott et al. 2021) and presented several promising candidate events (i.e., GW190519, GW190521, GW190602, GW190620, and GW190706) that are plotted in Figure 3 (see also e.g., Abbott et al. 2020c; Gerosa & Fishbach 2021; Baibhav et al. 2021). Moreover, GW170729 (Abbott et al. 2019), GW170817A (Zackay et al. 2021) and GW190412 (Abbott et al. 2020a) with  $M \sim 35 M_\odot$ ,  $\sim 40 M_\odot$ , and  $q \sim 0.28$  and  $\chi_{\text{eff}} \sim 0.37$ ,  $\sim 0.5$ , and  $\sim 0.25$ , respectively, also are promising candidates (e.g., Yang et al. 2019b; Gayathri et al. 2020; Gerosa et al. 2020). We find that most of the hierarchical merger candidates are consistent with the AGN channel because of the large chirp masses and high effective spins. Thus, most of the hierarchical merger candidate events detected by LIGO-Virgo (LIGO Scientific Collaboration et al. 2015; Acernese et al. 2015) may originate from the AGN channel if AGNs in all probability dominant the hierarchical BH merger rate (Yang et al. 2019b; Saavik Ford & McKernan 2022).

It is possible that GW190412 originated from SCs or AGNs. However, GW190412 has a component BH with the mass of  $\sim 8 M_\odot$  that should be a 1G BH, which implies it is more likely to come from AGNs because NG+1G mergers prefer to occur in AGNs. GW190521 (Abbott et al. 2020b) is in disfavor of originating from AGNs because of  $\chi_{\text{eff}}$  near zero; it has relatively symmetric masses with a total mass of  $\sim 150 M_\odot$ , which suggests it would be an NG+NG merger. Therefore, GW190521 should originate from SCs, but even within SCs, it is still an extremely rare case.

#### 4. DISCUSSION

The assumption that the mergers of NG+1G and NG+NG dominate the hierarchical merger rates of AGNs and SCs, respectively, relies on the efficiency of migration traps and mass segregation. Li (2022b) has shown that the NG+1G binaries dominate hierarchical BH mergers in AGNs with the percentage in hierarchical mergers is at least  $\sim 90\%$  by neglecting migration times and considering that the BHs reach the migration trap region once they align with their orbits with the AGN disk. In Li (2022a), we predicted that the branching ratio of the mergers of 2G+1G and 2G+2G in SCs is  $\geq 20$  by neglecting the pairing probability. However, this could go into reverse if the pairing probability is strongly in favor of equal-mass binaries because of mass segregation.

We expect to identify whether NG+NG or NG+1G dominates hierarchical mergers in SCs by the observation of future ground-based GW detectors, which is also a test for the efficiency of migration traps and mass segregation.

Generally, the initial BH mass function in dense stellar environment depends on metallicity (Arca Sedda et al. 2020; Fragione et al. 2020; Mapelli et al. 2021b) that we have not considered in our models. Most GCs are low-metallicity environments (Harris 1996), which therefore can form much more massive BHs (Vink et al. 2001; Spera & Mapelli 2017). Both low- and high-metallicity stars are in NSCs because of their complex history and various episodes of accretion and star formation (e.g., Antonini 2013). We also have ignored the increase in mass of BHs in AGN disks under accretion (Yi et al. 2018; Yang et al. 2020). These may change our results of masses slightly.

The kick velocities of merger remnants are sensitive to BH spins; low spins are in favor of the relatively small kick velocities imparted to merger remnants (Rodriguez et al. 2019; Fragione & Loeb 2021). Possibly, the occurrence of hierarchical mergers in young star clusters if the kick velocities are small enough (Gerosa & Fishbach 2021; Mapelli et al. 2021a,b). The rate of hierarchical mergers in SCs depends on the escape velocities of host clusters. Gerosa & Berti (2019) showed that the SC with an escape velocity of  $\geq 50 \text{ km s}^{-1}$  could populate the PI mass gap. Moreover, the results of Zevin & Holz (2022) indicated that there is a ‘cluster catastrophe’ of an abundance of high-mass mergers if the SCs with escape velocities of  $\sim 300 \text{ km s}^{-1}$  dominate the BBH merger rate. Therefore, the kick velocities between  $\sim 50 \text{ km s}^{-1}$  and  $\sim 300 \text{ km s}^{-1}$  are appropriate to hierarchical mergers in SCs, although Mahapatra et al. (2022) found that two of the subdominant peaks of the predictive BH mass spectrum are consistent with the 2G and 3G mergers with escape velocities of  $\sim 500 \text{ km s}^{-1}$ . Moreover, in our models, the hierarchical merger efficiency with  $\sim 50\%$  of the mergers being hierarchies would be too high if the SCs with escape velocities of  $\sim 500 \text{ km s}^{-1}$  dominate the BBH merger rate (see Table 2 in Appendix A).

The hierarchical merger rate in AGNs is determined by delay times (i.e., migration times) in our models. Because the kick velocities of merger remnants are always less than the escape velocity in AGN disks due to the large orbital velocities and the appropriate misalignment angle (Bogdanović et al. 2007; McKernan et al. 2012; Yi & Cheng 2019; McKernan et al. 2020). If migration times are short, then the fraction of hierarchical mergers can reach up to  $\sim 50\%$  in all three hierarchical branches (see Table 2 in Appendix A). Saavik Ford & McKernan (2022) predicted that the BBH merger rate in AGNs is larger than that of NSCs and contributes  $\sim 25\% - 80\%$  of the LIGO-Virgo measured rate of  $\sim 24 \text{ Gpc}^{-3} \text{ yr}^{-1}$ .

(The LIGO Scientific Collaboration et al. 2021b). Moreover, McKernan et al. (2020) found that  $\sim 80\%$ – $90\%$  of mergers occur away from migration traps, and  $\sim 10\%$ – $20\%$  of mergers occur at traps, which means most mergers occur within migration times. These show that multi-body interactions (Secunda et al. 2021; Wang et al. 2021; Samsing et al. 2022; Li et al. 2022) and/or the efficiency of migration traps (McKernan et al. 2012; Bellovary et al. 2016; Secunda et al. 2019; Pan & Yang 2021; Peng & Chen 2021) in AGN disks may play an important role if the efficiency of hierarchical mergers is overestimated by us, although we can constrain it by rising migration times.

## 5. CONCLUSIONS

In this paper, we compare hierarchical BH mergers in SCs and AGNs using simple models. We mainly focus on the differences of hierarchical mergers between SCs and AGNs, not on the differences within SCs or AGNs under different model parameters. In our models, the two dynamical BBH formation channels are distinguished by initial BH distributions in mass and spin, pairing probabilities, escape velocities, and delay times. We show that hierarchical mergers in mass and spin have significantly differences in between SCs and AGNs regardless of the model parameters. We stress that our estimates should be seen as upper limit because of neglecting multi-body interactions and the efficiency of migration traps and mass segregation. Our conclusions are as follows:

- The primary mass distribution of the hierarchical mergers in AGNs, with the peak of  $\sim 50 M_\odot$  and with wide ranges, is higher than that with the peak of  $\sim 13 M_\odot$  in SCs (see Figure 1). The hierarchical mergers in both AGNs and SCs can efficiently pollute the PI mass gap, but it is difficult to fill IMBHs for the cases with the maximum merger generation  $N_{\max}^G = 3$ . Compared with SCs, the hierarchical mergers in AGNs prefer asymmetric masses (see Figure 4 in Appendix B).
- The effective spin distribution of hierarchical mergers in SCs is symmetrical around zero as expected, in which  $\sim 50\%$  of the mergers have  $|\chi_{\text{eff}}| > 0.2$ , while that in AGNs is narrower and prefers positive values with the peak of  $\chi_{\text{eff}} \geq 0.3$  with the assistance of AGN disks (see Figure 2). The distribution of  $\chi_{\text{eff}}$  weakly depends on escape velocities and delay times. The effective precession parameter distribution with the peak of  $\chi_p \sim 0.66$  in SCs are much narrower than that in AGNs; the distribution of  $\chi_p$  in AGNs is flat, especially for NG+1G mergers, because of the assistance of AGN disks (see Figure 5 in Appendix C).
- The hierarchical BH merger rate in SCs strongly depends on the escape velocities of clusters, while that in AGNs depends on the delay times between subsequent

mergers. Compared with SCs, the fraction of hierarchical mergers in AGNs is higher with  $\sim 30\%$ – $50\%$ ; the percentage in SCs is  $\sim 10\%$ – $50\%$  that has great uncertainty determined by the escape velocities (see Table 2 in Appendix A). As a whole, BH hierarchical growth efficiency in AGNs should be much higher than the efficiency in SCs.

- Most of the hierarchical merger candidate events detected by LIGO-Virgo may originate from the AGN channel (see Figure 3). GW190412 is more likely to come from AGNs because of a small component BH mass. GW190521 should originate from SCs due to a significantly large total mass and relatively symmetric masses, but even within SCs, it is still an extremely rare case.

Our results in SCs and/or AGNs broadly agree with those in Rodriguez et al. (2019), Yang et al. (2019b), Fragione & Silk (2020), Tagawa et al. (2021a), and Mapelli et al. (2021a,b). We expect that with third-generation GW detectors in operation (Punturo et al. 2010a,b; Abbott et al. 2017), the increasing data on GW events will help us to constrain hierarchical mergers precisely in the two dynamical formation channels.



## ACKNOWLEDGMENTS

This work is supported by the National Natural Science Foundation of China (Grant No. 11773007) and the Guangxi Science Foundation (Grant No. 2018GXNSFFA281010).

## APPENDIX

## A. FRACTION OF EACH MERGER GENERATION

Table 2 lists the fraction of each merger generation of the three hierarchical branches for the eighteen models. The hierarchical mergers in AGNs are more efficient than that in SCs because almost all of the merger remnants could be retained in migration traps in AGN disks. The kick velocities of NG+NG merges are larger than the others and therefore their fractions of hierarchical mergers are relatively low in SCs.

## B. MASS RATIO DISTRIBUTION

In Section 3.1, we show the primary mass distribution of hierarchical mergers (see Figure 1). Here, we plot their probability density distribution of the mass ratios ( $q$ ) in Figure 4, which is broadly consistent with the results of Mahapatra et al. (2022) for SCs. We find that (on average) hierarchical mergers could lead to the formation of more asymmetric binaries in dynamical formation channels. Compared with NG+NG mergers, NG+1G mergers in both SCs and AGNs prefers unequal-mass binaries depending on hierarchical merger efficiency. Because the higher-generation mergers, the more extreme mass ratios for the branch of NG+1G. The mass ratio distribution of NG+ $\leq$ NG mergers is between NG+1G and NG+NG mergers. For NG+NG mergers, the distributions in SCs and AGNs are not very different. In SCs, the distribution of  $q$  of NG+1G mergers has large uncertainty, in which the distribution of the model of GC\_5 is the highest at the low- $q$  end. The hierarchical mergers in AGNs would be more asymmetric than that in SCs, if NG+1G and NG+NG mergers dominate the hierarchical BH merger rates in AGNs and SCs, respectively.

## C. EFFECTIVE PRECESSION PARAMETER DISTRIBUTION

In Section 3.1, we show the effective spin distribution of hierarchical mergers (see Figure 2). Here, we show the probability density distribution of the effective precession parameters ( $\chi_p$ ) of hierarchical BH mergers in Figure 5, where  $\chi_p = \max[\chi_1 \sin \theta_1, \chi_2 \sin \theta_2 q(4q + 3)/(4 + 3q)]$ . We see that the effective precession parameter distributions with the peak of  $\chi_p \sim 0.66$  in SCs are much narrower than that in AGNs. The distribution of  $\chi_p$  in AGNs is flat, especially for NG+1G mergers, because gas accretion tends to torque the BH spin into alignment with the AGN disk. The results of the distributions of  $\chi_p$  in SCs and/or AGNs agree with those in Baibhav et al. (2021) and Tagawa et al. (2021a).

**Table 2.** The fraction of each merger generation of the three hierarchical branches for the eighteen models.

Model	Branch	1G	2G	3G	4G	5G	6G	7G	8G	9G	10G
SC_1	NG+1G	0.751	0.24	0.007	$9 \times 10^{-4}$	$3 \times 10^{-4}$	$1 \times 10^{-4}$	$7 \times 10^{-5}$	$3 \times 10^{-5}$	$2 \times 10^{-5}$	$8 \times 10^{-6}$
	NG+NG	0.753	0.241	0.006	$1 \times 10^{-4}$	$6 \times 10^{-6}$	0	0	0	0	0
	NG+ $\leq$ NG	0.752	0.24	0.007	$5 \times 10^{-4}$	$1 \times 10^{-4}$	$4 \times 10^{-5}$	$2 \times 10^{-5}$	$8 \times 10^{-6}$	0	0
SC_2	NG+1G	0.907	0.093	$3 \times 10^{-4}$	$1 \times 10^{-5}$	$7 \times 10^{-6}$	0	0	0	0	0
	NG+NG	0.907	0.093	$2 \times 10^{-4}$	$7 \times 10^{-6}$	0	0	0	0	0	0
	NG+ $\leq$ NG	0.907	0.093	$3 \times 10^{-4}$	$7 \times 10^{-6}$	0	0	0	0	0	0
SC_3	NG+1G	0.614	0.307	0.051	0.015	0.007	0.004	0.002	$9 \times 10^{-4}$	$5 \times 10^{-4}$	$2 \times 10^{-4}$
	NG+NG	0.636	0.318	0.039	0.006	$7 \times 10^{-4}$	$9 \times 10^{-5}$	$8 \times 10^{-6}$	$4 \times 10^{-6}$	0	0
	NG+ $\leq$ NG	0.622	0.311	0.047	0.011	0.004	0.002	0.001	$5 \times 10^{-4}$	$2 \times 10^{-4}$	$1 \times 10^{-4}$
SC_4	NG+1G	0.559	0.279	0.087	0.038	0.019	0.009	0.005	0.002	0.001	$6 \times 10^{-4}$
	NG+NG	0.602	0.301	0.072	0.019	0.006	0.001	$2 \times 10^{-4}$	$4 \times 10^{-5}$	$1 \times 10^{-5}$	$4 \times 10^{-6}$
	NG+ $\leq$ NG	0.571	0.286	0.082	0.031	0.015	0.008	0.004	0.002	0.001	$5 \times 10^{-4}$
SC_5	NG+1G	0.501	0.25	0.125	0.063	0.031	0.016	0.009	0.004	0.002	0.001
	NG+NG	0.532	0.266	0.115	0.052	0.021	0.009	0.003	0.001	$4 \times 10^{-4}$	$2 \times 10^{-4}$
	NG+ $\leq$ NG	0.503	0.252	0.123	0.062	0.031	0.015	0.008	0.004	0.002	0.001
SC_6	NG+1G	0.751	0.24	0.008	$9 \times 10^{-4}$	$3 \times 10^{-4}$	$1 \times 10^{-4}$	$6 \times 10^{-5}$	$3 \times 10^{-5}$	$1 \times 10^{-5}$	$8 \times 10^{-6}$
	NG+NG	0.753	0.241	0.006	$1 \times 10^{-4}$	$6 \times 10^{-6}$	0	0	0	0	0
	NG+ $\leq$ NG	0.752	0.24	0.007	$5 \times 10^{-4}$	$1 \times 10^{-4}$	$4 \times 10^{-5}$	$2 \times 10^{-5}$	$6 \times 10^{-6}$	0	0
SC_7	NG+1G	0.751	0.24	0.007	$9 \times 10^{-4}$	$3 \times 10^{-4}$	$1 \times 10^{-4}$	$6 \times 10^{-5}$	$3 \times 10^{-5}$	$1 \times 10^{-5}$	$4 \times 10^{-6}$
	NG+NG	0.753	0.241	0.006	$2 \times 10^{-4}$	$6 \times 10^{-6}$	$6 \times 10^{-6}$	0	0	0	0
	NG+ $\leq$ NG	0.752	0.24	0.007	$5 \times 10^{-4}$	$1 \times 10^{-4}$	$3 \times 10^{-5}$	$1 \times 10^{-5}$	$6 \times 10^{-6}$	0	0
SC_8	NG+1G	0.691	0.296	0.01	0.002	$6 \times 10^{-4}$	$3 \times 10^{-4}$	$2 \times 10^{-4}$	$8 \times 10^{-5}$	$4 \times 10^{-5}$	$2 \times 10^{-5}$
	NG+NG	0.695	0.298	0.007	$2 \times 10^{-4}$	$6 \times 10^{-6}$	0	0	0	0	0
	NG+ $\leq$ NG	0.693	0.297	0.009	0.001	$2 \times 10^{-4}$	$8 \times 10^{-5}$	$3 \times 10^{-5}$	$2 \times 10^{-5}$	$7 \times 10^{-6}$	0
SC_9	NG+1G	0.659	0.329	0.01	0.001	$4 \times 10^{-4}$	$2 \times 10^{-4}$	$1 \times 10^{-4}$	$5 \times 10^{-5}$	$2 \times 10^{-5}$	$1 \times 10^{-5}$
	NG+NG	0.661	0.331	0.008	$2 \times 10^{-4}$	$6 \times 10^{-6}$	0	0	0	0	0
	NG+ $\leq$ NG	0.660	0.330	0.009	$8 \times 10^{-4}$	$2 \times 10^{-4}$	$6 \times 10^{-5}$	$2 \times 10^{-5}$	$9 \times 10^{-6}$	$6 \times 10^{-6}$	0
SC_10	NG+1G	0.853	0.142	0.004	$5 \times 10^{-4}$	$2 \times 10^{-4}$	$8 \times 10^{-5}$	$4 \times 10^{-5}$	$2 \times 10^{-5}$	$9 \times 10^{-6}$	0
	NG+NG	0.855	0.142	0.003	$8 \times 10^{-5}$	0	0	0	0	0	0
	NG+ $\leq$ NG	0.854	0.142	0.004	$3 \times 10^{-4}$	$9 \times 10^{-5}$	$2 \times 10^{-5}$	$8 \times 10^{-6}$	0	0	0
AGN_1	NG+1G	0.501	0.25	0.125	0.062	0.031	0.016	0.008	0.004	0.002	0.001
	NG+NG	0.501	0.25	0.125	0.062	0.031	0.016	0.008	0.004	0.002	0.001
	NG+ $\leq$ NG	0.501	0.25	0.125	0.062	0.031	0.016	0.008	0.004	0.002	0.001
AGN_2	NG+1G	0.501	0.25	0.125	0.062	0.031	0.016	0.008	0.004	0.002	0.001
	NG+NG	0.506	0.253	0.126	0.063	0.029	0.013	0.006	0.003	0.001	$5 \times 10^{-4}$
	NG+ $\leq$ NG	0.501	0.25	0.125	0.062	0.031	0.016	0.008	0.004	0.002	0.001
AGN_3	NG+1G	0.501	0.25	0.125	0.063	0.031	0.016	0.008	0.004	0.002	0.001
	NG+NG	0.501	0.25	0.125	0.063	0.031	0.016	0.008	0.004	0.002	0.001
	NG+ $\leq$ NG	0.501	0.25	0.125	0.063	0.031	0.016	0.008	0.004	0.002	0.001
AGN_4	NG+1G	0.552	0.257	0.116	0.049	0.012	0.006	0.001	$6 \times 10^{-5}$	0	0
	NG+NG	0.552	0.257	0.116	0.049	0.019	0.006	0.001	$5 \times 10^{-5}$	0	0
	NG+ $\leq$ NG	0.552	0.257	0.116	0.049	0.019	0.006	0.001	$6 \times 10^{-5}$	$4 \times 10^{-6}$	0
AGN_5	NG+1G	0.668	0.255	0.071	0.006	0	0	0	0	0	0
	NG+NG	0.667	0.255	0.071	0.006	0	0	0	0	0	0
	NG+ $\leq$ NG	0.668	0.255	0.071	0.006	0	0	0	0	0	0

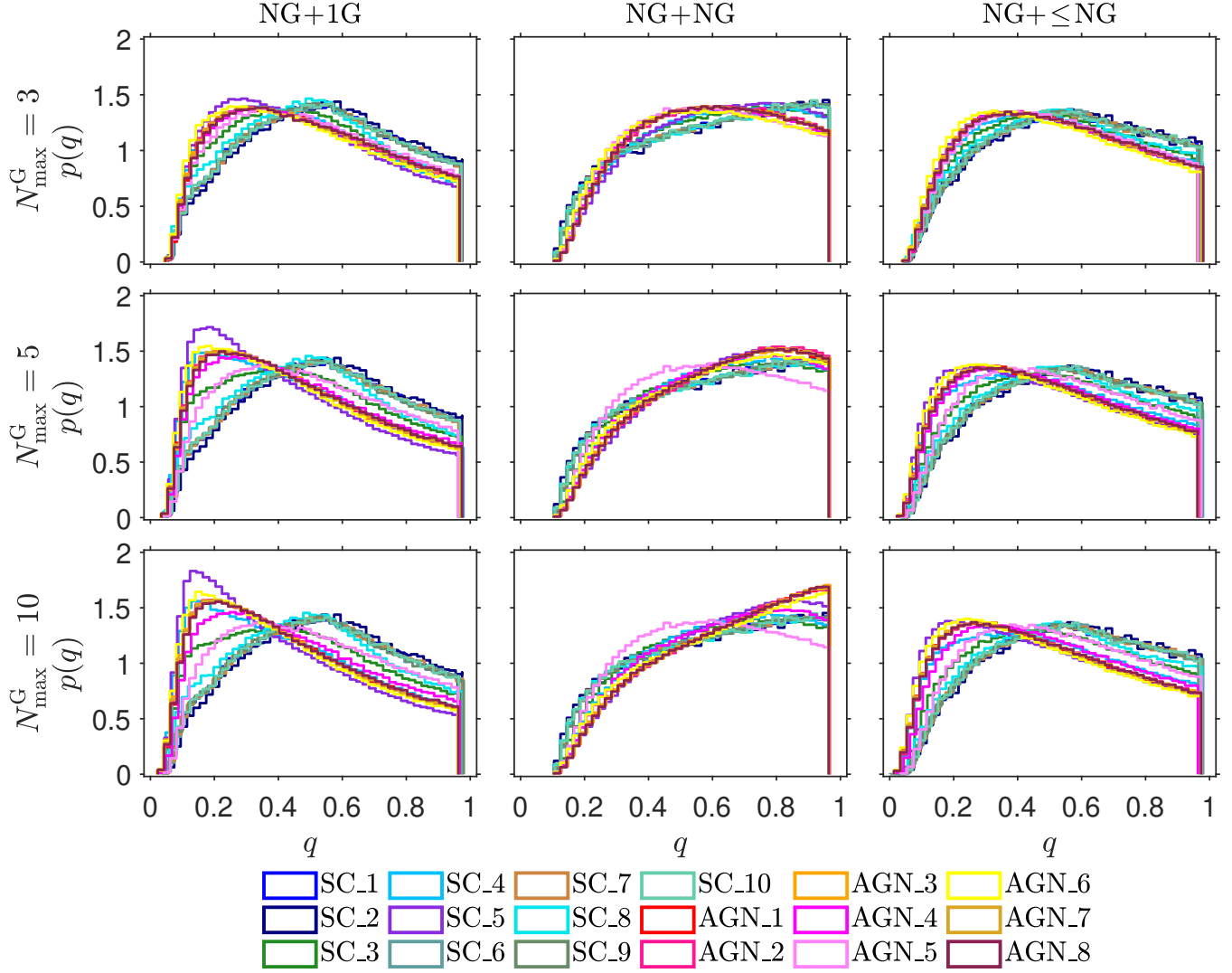
Continued on next page

Table 2 – continued from previous page

Model	Branch	1G	2G	3G	4G	5G	6G	7G	8G	9G	10G
AGN_6	NG+1G	0.501	0.25	0.125	0.062	0.031	0.016	0.008	0.004	0.002	0.001
	NG+NG	0.501	0.25	0.125	0.062	0.031	0.016	0.008	0.004	0.002	0.001
	NG+ $\leq$ NG	0.501	0.25	0.125	0.062	0.031	0.016	0.008	0.004	0.002	0.001
AGN_7	NG+1G	0.501	0.25	0.125	0.062	0.031	0.016	0.008	0.004	0.002	0.001
	NG+NG	0.501	0.25	0.125	0.062	0.031	0.016	0.008	0.004	0.002	0.001
	NG+ $\leq$ NG	0.501	0.25	0.125	0.062	0.031	0.016	0.008	0.004	0.002	0.001
AGN_8	NG+1G	0.501	0.25	0.125	0.062	0.031	0.016	0.008	0.004	0.002	0.001
	NG+NG	0.501	0.25	0.125	0.062	0.031	0.016	0.008	0.004	0.002	0.001
	NG+ $\leq$ NG	0.501	0.25	0.125	0.062	0.031	0.016	0.008	0.004	0.002	0.001

## REFERENCES

- Abbott, B. P., Abbott, R., Abbott, T. D., et al. 2017, *Classical and Quantum Gravity*, 34, 044001
- . 2019, *Physical Review X*, 9, 031040
- Abbott, R., Abbott, T. D., Abraham, S., et al. 2020a, *PhRvD*, 102, 043015
- . 2020b, *PhRvL*, 125, 101102
- . 2020c, *ApJL*, 900, L13
- . 2021, *Physical Review X*, 11, 021053
- Acernese, F., Agathos, M., Agatsuma, K., et al. 2015, *Classical and Quantum Gravity*, 32, 024001
- Antonini, F. 2013, *ApJ*, 763, 62
- Antonini, F., & Rasio, F. A. 2016, *ApJ*, 831, 187
- Arca Sedda, M., Mapelli, M., Spera, M., Benacquista, M., & Giacobbo, N. 2020, *ApJ*, 894, 133
- Baibhav, V., Berti, E., Gerosa, D., Mould, M., & Wong, K. W. K. 2021, *PhRvD*, 104, 084002
- Barausse, E., Morozova, V., & Rezzolla, L. 2012, *ApJ*, 758, 63
- Bartos, I., Kocsis, B., Haiman, Z., & Márka, S. 2017, *ApJ*, 835, 165
- Bellovary, J. M., Mac Low, M.-M., McKernan, B., & Ford, K. E. S. 2016, *ApJL*, 819, L17
- Bogdanović, T., Reynolds, C. S., & Miller, M. C. 2007, *ApJL*, 661, L147
- Campanelli, M., Lousto, C., Zlochower, Y., & Merritt, D. 2007, *ApJL*, 659, L5
- Di Carlo, U. N., Mapelli, M., Bouffanais, Y., et al. 2020, *MNRAS*, 497, 1043
- Doctor, Z., Wysocki, D., O’Shaughnessy, R., Holz, D. E., & Farr, B. 2020, *ApJ*, 893, 35
- Dominik, M., Belczynski, K., Fryer, C., et al. 2012, *ApJ*, 759, 52
- Fragione, G., Kocsis, B., Rasio, F. A., & Silk, J. 2022, *ApJ*, 927, 231
- Fragione, G., & Loeb, A. 2021, *MNRAS*, 502, 3879
- Fragione, G., Loeb, A., & Rasio, F. A. 2020, *ApJL*, 902, L26
- Fragione, G., & Silk, J. 2020, *MNRAS*, 498, 4591
- Gayathri, V., Bartos, I., Haiman, Z., et al. 2020, *ApJL*, 890, L20
- Gerosa, D., & Berti, E. 2019, *PhRvD*, 100, 041301
- Gerosa, D., & Fishbach, M. 2021, *Nature Astronomy*, 5, 749
- Gerosa, D., Giacobbo, N., & Vecchio, A. 2021, *ApJ*, 915, 56
- Gerosa, D., & Kesden, M. 2016, *PhRvD*, 93, 124066
- Gerosa, D., Vitale, S., & Berti, E. 2020, *PhRvL*, 125, 101103
- González Prieto, E., Kremer, K., Fragione, G., et al. 2022, *arXiv e-prints*, arXiv:2208.07881
- Harris, W. E. 1996, *AJ*, 112, 1487
- Heger, A., Fryer, C. L., Woosley, S. E., Langer, N., & Hartmann, D. H. 2003, *ApJ*, 591, 288
- Hofmann, F., Barausse, E., & Rezzolla, L. 2016, *ApJL*, 825, L19
- Kimball, C., Talbot, C., Berry, C. P. L., et al. 2020, *ApJ*, 900, 177
- . 2021, *ApJL*, 915, L35
- Kroupa, P. 2001, *MNRAS*, 322, 231
- Li, G.-P. 2022a, *A&A*, 666, A194
- . 2022b, *PhRvD*, 105, 063006
- Li, J., Dempsey, A. M., Li, H., Lai, D., & Li, S. 2022, *arXiv e-prints*, arXiv:2211.10357
- LIGO Scientific Collaboration, Aasi, J., Abbott, B. P., et al. 2015, *Classical and Quantum Gravity*, 32, 074001
- Liu, B., & Lai, D. 2021, *MNRAS*, 502, 2049
- Mahapatra, P., Gupta, A., Favata, M., Arun, K. G., & Sathyaprakash, B. S. 2021, *ApJL*, 918, L31
- . 2022, *arXiv e-prints*, arXiv:2209.05766
- Mapelli, M., Santoliquido, F., Bouffanais, Y., et al. 2021a, *Symmetry*, 13, 1678
- Mapelli, M., Dall’Amico, M., Bouffanais, Y., et al. 2021b, *MNRAS*, 505, 339
- McKernan, B., Ford, K. E. S., Lyra, W., & Perets, H. B. 2012, *MNRAS*, 425, 460



**Figure 4.** Same as Figure 1, but the probability density distribution of the mass ratios ( $q$ ) of hierarchical BH mergers.

McKernan, B., Ford, K. E. S., O’Shaughnessy, R., & Wysocki, D. 2020, *MNRAS*, 494, 1203

McKernan, B., Ford, K. E. S., Bellovary, J., et al. 2018, *ApJ*, 866, 66

Mould, M., Gerosa, D., & Taylor, S. R. 2022, *Phys. Rev. D*, 106, 103013

Nony, T., Robitaille, J. F., Motte, F., et al. 2021, *A&A*, 645, A94

Pan, Z., & Yang, H. 2021, *PhRvD*, 103, 103018

Pavlík, V., & Vesperini, E. 2022, *MNRAS*, 515, 1830

Peng, P., & Chen, X. 2021, *MNRAS*, 505, 1324

Punturo, M., Abernathy, M., Acernese, F., et al. 2010a, *Classical and Quantum Gravity*, 27, 194002

—. 2010b, *Classical and Quantum Gravity*, 27, 084007

Quinlan, G. D., & Shapiro, S. L. 1987, *ApJ*, 321, 199

Rodriguez, C. L., Zevin, M., Amaro-Seoane, P., et al. 2019, *PhRvD*, 100, 043027

Saavik Ford, K. E., & McKernan, B. 2022, *MNRAS*, arXiv:2109.03212

Samsing, J., Bartos, I., D’Orazio, D. J., et al. 2022, *Nature*, 603, 237

Scaria, K. K., & Bappu, M. K. V. 1981, *Journal of Astrophysics and Astronomy*, 2, 215

Secunda, A., Bellovary, J., Mac Low, M.-M., et al. 2019, *ApJ*, 878, 85

Secunda, A., Hernandez, B., Goodman, J., et al. 2021, *ApJL*, 908, L27

Spera, M., & Mapelli, M. 2017, *MNRAS*, 470, 4739

Tagawa, H., Haiman, Z., Bartos, I., Kocsis, B., & Omukai, K. 2021a, *MNRAS*, 507, 3362

Tagawa, H., Haiman, Z., & Kocsis, B. 2020, *ApJ*, 898, 25

Tagawa, H., Kocsis, B., Haiman, Z., et al. 2021b, *ApJ*, 908, 194

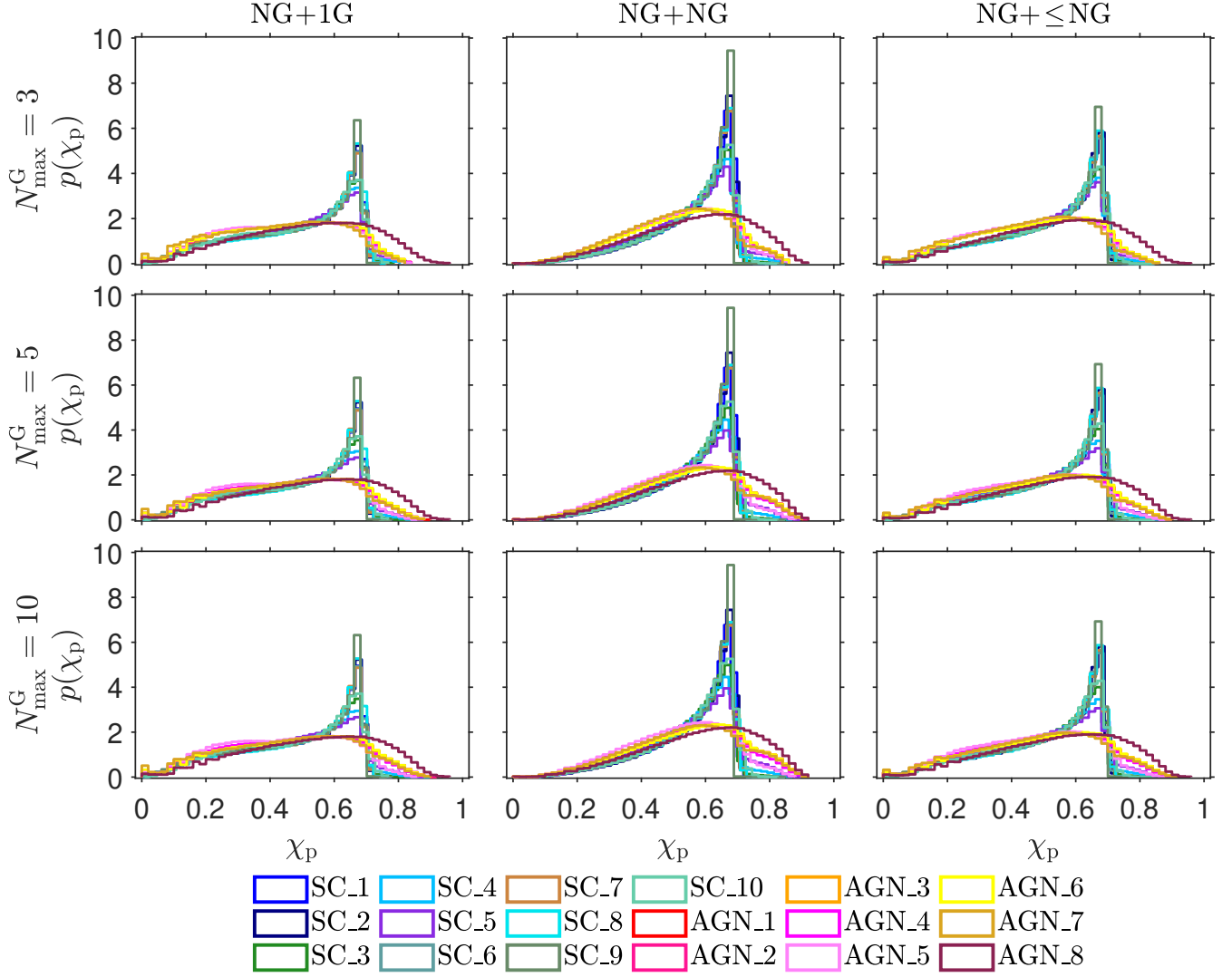


**Figure 5.** Same as Figure 1, but the probability density distribution of the effective precession parameters ( $\chi_p$ ) of hierarchical BH mergers.

The LIGO Scientific Collaboration, the Virgo Collaboration, the KAGRA Collaboration, et al. 2021a, arXiv e-prints, arXiv:2111.03606  
 —. 2021b, arXiv e-prints, arXiv:2111.03634  
 Tiwari, V. 2021, *Classical and Quantum Gravity*, 38, 155007  
 —. 2022, *ApJ*, 928, 155  
 Varma, V., Biscoveanu, S., Islam, T., et al. 2022, *PhRvL*, 128, 191102  
 Vink, J. S., de Koter, A., & Lamers, H. J. G. L. M. 2001, *A&A*, 369, 574

Vitral, E., Kremer, K., Libralato, M., Mamon, G. A., & Bellini, A. 2022, *MNRAS*, 514, 806  
 Wang, Y.-H., McKernan, B., Ford, S., et al. 2021, *ApJL*, 923, L23  
 Woosley, S. E., Blinnikov, S., & Heger, A. 2007, *Nature*, 450, 390  
 Yang, Y., Bartos, I., Haiman, Z., et al. 2019a, *ApJ*, 876, 122  
 Yang, Y., Gayathri, V., Bartos, I., et al. 2020, *ApJL*, 901, L34  
 Yang, Y., Bartos, I., Gayathri, V., et al. 2019b, *PhRvL*, 123, 181101  
 Yi, S.-X., & Cheng, K. S. 2019, *ApJL*, 884, L12  
 Yi, S.-X., Cheng, K. S., & Taam, R. E. 2018, *ApJL*, 859, L25  
 Zackay, B., Dai, L., Venumadhav, T., Roulet, J., & Zaldarriaga, M. 2021, *PhRvD*, 104, 063030  
 Zevin, M., & Holz, D. E. 2022, *ApJL*, 935, L20